



This is a repository copy of *Iron loss in permanent-magnet brushless AC machines under maximum torque per ampere and flux weakening control* .

White Rose Research Online URL for this paper:  
<http://eprints.whiterose.ac.uk/872/>

---

**Article:**

Zhu, Z.Q., Chen, Y.S. and Howe, D. (2002) Iron loss in permanent-magnet brushless AC machines under maximum torque per ampere and flux weakening control. IEEE Transactions on Magnetics, 38 (5 (Par)). pp. 3285-3287. ISSN 0018-9464

<https://doi.org/10.1109/TMAG.2002.802296>

---

**Reuse**

Unless indicated otherwise, fulltext items are protected by copyright with all rights reserved. The copyright exception in section 29 of the Copyright, Designs and Patents Act 1988 allows the making of a single copy solely for the purpose of non-commercial research or private study within the limits of fair dealing. The publisher or other rights-holder may allow further reproduction and re-use of this version - refer to the White Rose Research Online record for this item. Where records identify the publisher as the copyright holder, users can verify any specific terms of use on the publisher's website.

**Takedown**

If you consider content in White Rose Research Online to be in breach of UK law, please notify us by emailing [eprints@whiterose.ac.uk](mailto:eprints@whiterose.ac.uk) including the URL of the record and the reason for the withdrawal request.



[eprints@whiterose.ac.uk](mailto:eprints@whiterose.ac.uk)  
<https://eprints.whiterose.ac.uk/>

# Iron Loss in Permanent-Magnet Brushless AC Machines Under Maximum Torque Per Ampere and Flux Weakening Control

Z. Q. Zhu, *Senior Member, IEEE*, Y. S. Chen, and D. Howe

**Abstract**—The airgap flux density distribution, flux density loci in the stator core, and the associated iron loss in two topologies of brushless ac motor, having a surface-mounted magnet rotor and an interior-mounted magnet rotor, respectively, are investigated when operated under maximum torque per ampere control in the constant torque mode and maximum power control in the flux-weakening mode. It is shown that whilst the interior magnet topology is known to be eminently suitable for flux-weakening operation, due to its high demagnetization withstand capability, its iron loss can be significantly higher than for a surface-mounted magnet machine.

**Index Terms**—Flux-weakening, permanent-magnet machines, iron loss.

## I. INTRODUCTION

**P**ERMANENT-MAGNET brushless ac machines, when employed in applications such as electric vehicles and spindle drives, are operated under both constant torque and constant power modes. However, whilst the influence of machine parameters on the operational characteristics has been researched extensively [1], [2], relatively little has been reported on the influence of the control strategy and machine topology on the iron loss. However, the iron loss requires careful consideration, particularly under high-speed, flux-weakening control [3]. Most investigations, however, consider only the no-load iron loss [4], [5]. This paper investigates the airgap flux density distribution, the flux density loci in the stator core, and the associated iron loss in two brushless ac motor topologies, having a surface-mounted magnet rotor and an interior-mounted magnet rotor, respectively, when operated under maximum torque per ampere control in the constant torque mode and maximum power control in the flux-weakening mode.

## II. MOTORS AND AIRGAP FIELD DISTRIBUTIONS

In vector-controlled brushless ac drives, the stator phase currents are transformed to  $d$  and  $q$  axis currents in the rotor frame and controlled according to optimal current profiles in order to obtain the required magnitude of flux and torque, respectively. In the constant torque operating range, maximum torque per ampere control is widely used [1] for a surface-mounted magnet motor, maximum torque per ampere control results in zero  $d$  axis current, whilst for an interior magnet motor with saliency, maximum torque per ampere control results in a negative  $d$  axis

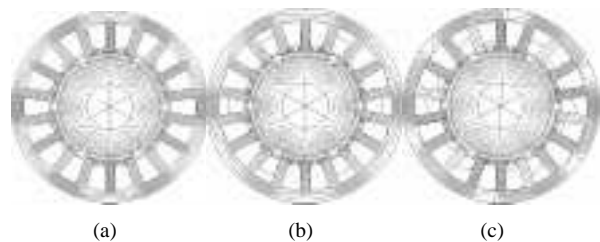


Fig. 1. Field distribution in surface-mounted magnet motor. (a) Open-circuit. (b) On-load ( $I_d = -4$  A,  $I_q = 0$ ). (c) On-load ( $I_d = 0$ ,  $I_q = 4$  A).

current in order to realize the reluctance torque component. In the flux-weakening (constant power) operating range, the  $d$  axis current progressively increases as the speed increases, while the  $q$  axis current reduces. The optimal  $d$  and  $q$  axis current profiles fully utilize the inverter capability, whilst maximizing the output power and torque. When the ratio of  $\omega L_d I_r / E \approx 1$ , where  $\omega$  is the angular speed,  $L_d$  is the  $d$  axis inductance,  $E$  is the phase back-emf, and  $I_r$  is the rated phase current, maximum flux-weakening capability (defined as the ratio of the maximum achievable speed to the base-speed) is achieved, being infinite in theory [2]. In this investigation, two 1.3 kW, three-phase permanent-magnet brushless ac motors having identical stators, with six poles, 18 slots, and an overlapping stator winding, but different rotors, viz. with surface-mounted magnets and interior-mounted magnets, and a ratio of  $\omega L_d I_r / E$  of 0.45 and 0.61, respectively, were considered. The dc-link voltage  $U_{dc} = 285$  V,  $I_r = 4$  A (peak), and the base-speed  $\approx 1700$  r/min. The motors were designed to have the same torque capability at base-speed. Hence, due to its saliency, the interior-mounted magnet motor produces a lower back-emf (93% of that for the surface-mounted magnet motor). The field distributions on open-circuit and at rated current (with rated  $q$  axis current, i.e.,  $I_d = 0$ ,  $I_q = 4$  A, and rated  $d$  axis current, i.e.,  $I_d = -4$  A,  $I_q = 0$ ) are shown in Figs. 1–4 for both motors.

The open-circuit airgap field distribution in both motors is similar, in that they have similar amplitudes and are modulated by the relatively wide stator slot openings (2.5 mm). The amplitudes of the  $d$  and  $q$  axis armature reaction fields in the surface-mounted magnet motor are also more or less similar, the armature reaction field being relatively weak due to the large effective airgap. For example, the average magnet working point reduces by  $\sim 0.1$  T under the influence of the  $d$  axis armature reaction field, the magnets being uniformly demagnetized throughout their volume, whilst the  $q$  axis armature reaction field demagnetizes only one side of each magnet. Due to the relatively small airgap, armature reaction in the interior magnet

Manuscript received February 14, 2002; revised May 9, 2002.

The authors are with the Department of Electronic and Electrical Engineering, University of Sheffield, Sheffield S1 3JD, U.K. (e-mail: Z.Q.Zhu@sheffield.ac.uk; S.J.Gawthorpe@sheffield.ac.uk).

Digital Object Identifier 10.1109/TMAG.2002.802296.

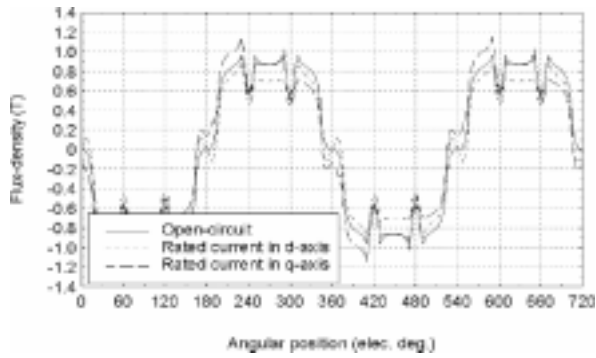


Fig. 2. Airgap field distribution in surface-mounted magnet motor.

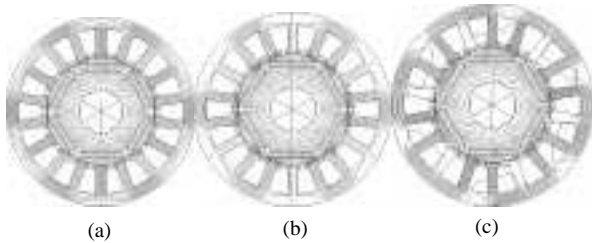


Fig. 3. Field distributions in interior magnet motor. (a) Open-circuit. (b) On-load ( $I_d = -4$  A,  $I_q = 0$ ). (c) On-load ( $I_d = 0$ ,  $I_q = 4$  A).

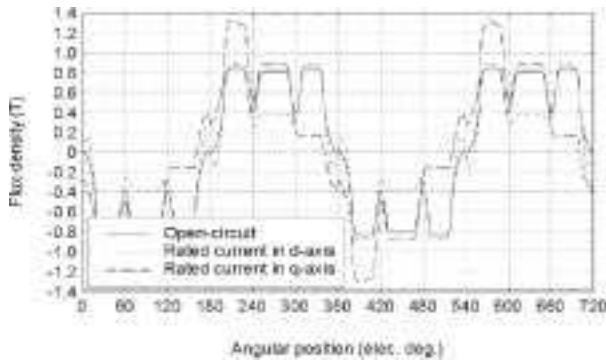
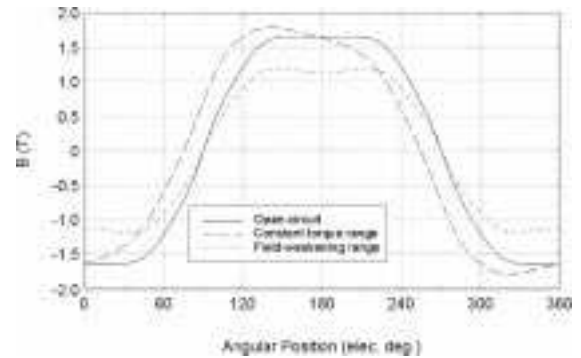


Fig. 4. Airgap field distribution in interior-magnet motor.

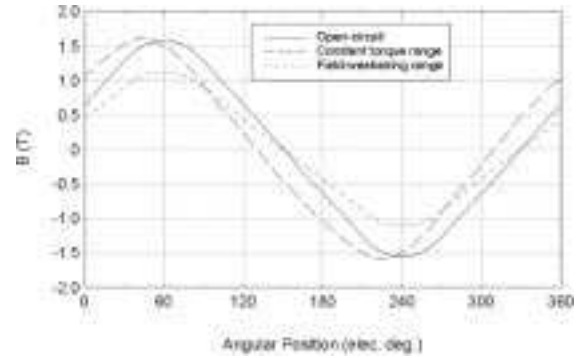
motor is much more significant, a large proportion of the  $d$  axis armature reaction flux passing through the rotor inter-pole regions, whilst the majority of the  $q$  axis armature reaction flux passes through the rotor iron rather than through the magnets. Thus, the effect of the  $d$  axis armature reaction field on the working point of the magnets, and hence, the potential for partial irreversible demagnetization, is greatly reduced. As will be observed from Figs. 2 and 4, the on-load airgap field contains significant harmonics, particularly in the interior-magnet motor. Thus, the on-load stator iron loss in the interior-magnet motor will be significantly higher than that in the surface-mounted magnet motor.

### III. IRON LOSS

The stator iron loss is calculated by finite-element analysis. By a well-developed and validated technique based on the finite-element method and experimentally determined loss coefficients for the stator lamination material [3]. It calculates the hysteresis, eddy current, and excess components of iron loss density on an element-by-element basis from flux density waveforms derived from a series of two-dimensional magnetostatic

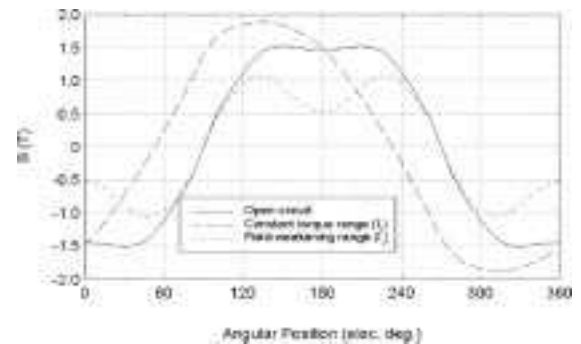


(a)

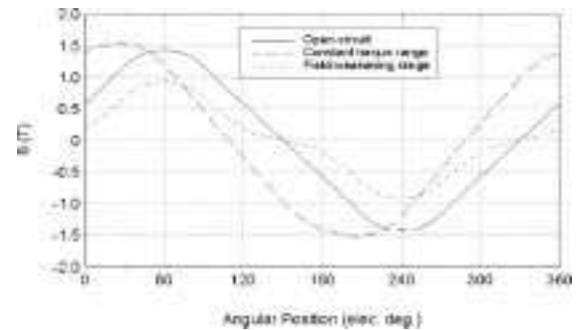


(b)

Fig. 5. Flux density waveforms in surface-mounted magnet motor. (a) Tooth. (b) Yoke. (Constant torque range: rated  $q$  axis current; flux-weakening range: rated  $d$  axis current).



(a)



(b)

Fig. 6. Flux density waveforms in interior-magnet motor. (a) Tooth. (b) Yoke. (Constant torque range: rated  $q$  axis current; flux-weakening range: rated  $d$  axis current)

field solutions as the rotor is rotated  $180^\circ$  elec. In the motors under consideration, the lamination thickness = 0.35 mm, mass

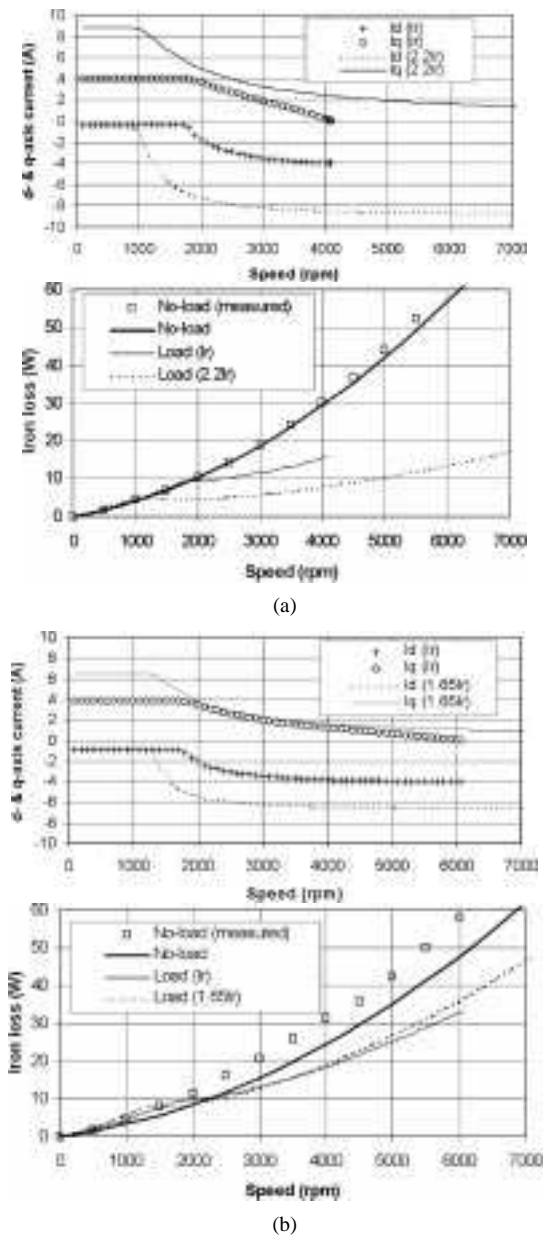


Fig. 7. Variation of iron loss in surface-mounted and interior-mounted magnet motors. (a) Surface-mounted magnet motor. (b) Interior-mounted magnet motor.

density =  $7650 \text{ kg/m}^3$ , resistivity =  $46 \times 10^{-8} \Omega \cdot \text{m}$ , and the hysteresis, eddy current, and excess loss coefficients are  $K_h = 1.71 \times 10^{-2}$ ,  $\alpha = 2.12$ , and  $K_e = 4.39 \times 10^{-5}$ . Figs. 5 and 6 show flux density waveforms in a stator tooth and the stator back-iron when both motors are on open-circuit and when the stator winding carries rated  $d$  and  $q$  axis currents. As will be seen, they are essentially alternating fluxes. However, the flux loci at the back of a tooth and at the tooth tips are essentially rotating, the resultant iron loss density then being the sum of the iron loss densities associated with the orthogonal alternating radial and circumferential flux components. As will be seen, the influence of armature reaction on the flux density waveforms is more significant in the interior-magnet motor.

The predicted stator open-circuit iron loss for both motors are compared with measured results in Fig. 7. The measured loss was determined by segregating loss components, simply

by measuring the power when the motor is run up to the required speed by a coupled motor, and subtracting the mechanical loss when the motor has a dummy nonmagnetic rotor and run up to the same speed. The surface-mounted magnet motor has a slightly higher open-circuit iron loss than the interior-magnet motor since its back-emf, and stator flux density, is higher. It should also be noted that the measured loss of the interior-magnet motor is slightly higher than predicted, due to the smaller effective airgap, which results in a loss induced by field harmonics in the laminated rotor poles.

Also shown in Fig. 7 are the  $d$  and  $q$  axis current profiles for maximum torque per ampere and flux-weakening control [1] with  $I_r = 4 \text{ A}$ , together with current profiles for infinite flux-weakening capability [2], when  $\omega L_d I_r / E = 1$ , which equates to currents of  $2.2I_r$  and  $1.65I_r$  for the surface-mounted and interior-magnet motors, respectively. The resulting iron loss was again deduced from magnetostatic field solutions, as instantaneous phase currents are assigned according to the rotor position. The variation of the stator iron loss with speed for both motors when they are operated with optimal  $d$  and  $q$  axis current profiles corresponding to rated current, as well as with the profiles corresponding to infinite flux-weakening, are shown in Fig. 7. As will be seen, the iron loss in the constant torque range is slightly higher than the iron loss on open-circuit. In the constant power, flux-weakening range, however, the iron loss becomes progressively lower than the open circuit value. However, the iron loss of the interior-magnet motor remains significantly higher than that of the surface-mounted magnet motor, due to the higher harmonic content in the armature reaction field. This is further highlighted by the fact that when the current in the surface-mounted magnet motor is increased to  $2.2I_r$ , a further significant reduction in the iron loss occurs in the flux-weakening range. When the current is increased to  $1.65I_r$  in the interior-magnet motor, the iron loss increases slightly in the flux-weakening range due to the armature reaction field harmonics.

#### IV. CONCLUSION

The stator iron loss in brushless ac motors, having a surface-mounted magnet rotor and an interior-mounted magnet rotor, respectively, has been investigated under both constant torque and constant power operating modes. Whilst the interior-magnet motor facilitates extended flux-weakening operation, its iron loss can be significantly higher in the flux-weakening operating range.

#### REFERENCES

- [1] S. Morimoto, M. Sanada, and Y. Takeda, "Wide-speed operation of interior permanent magnet synchronous motors with high-performance current regulator," *IEEE Trans. Industry Applicat.*, vol. 30, pp. 920–926, Jul.-Aug. 1994.
- [2] W. L. Soong and T. J. E. Miller, "Field-weakening performance of brushless synchronous AC motor drives," *Proc. Inst. Elect. Eng. B*, vol. 141, pp. 331–340, 1994.
- [3] B. Stumberger, B. Hribernik, and V. Gorican, "Flux distortion and iron losses in flux-weakened permanent magnet synchronous motor," *J. Magn. Mater.*, vol. 215–216, pp. 753–755, 2000.
- [4] K. Atallah, Z. Q. Zhu, and D. Howe, "An improved method for predicting iron losses in brushless permanent magnet drives," *IEEE Trans. Magn.*, vol. 28, pp. 2997–2999, Sept. 1992.
- [5] K. J. Tseng and S. B. Wee, "Analysis of flux distribution and core losses in interior permanent magnet motor," *IEEE Trans. Energy Conversion*, vol. 14, pp. 969–975, Dec. 1999.